# Solving partial differential equations with finite difference methods

D. D. Q. Ng
*Level 6 MSci. Laboratory, H. H. Wills Physics Laboratory, University of Bristol, BS8 1TL, UK*
(Dated: November 24, 2019)

Here the Gauss-Seidel method is first used to solved for the Laplace equation of a line charge in a partially grounded box as a known case, and in addition the Jacobi method is also used for a parallel plate capacitor. A convergence condition is chosen and the discussion of the sensitivity of solutions to the choice of convergence condition and grid density is also provided. Secondly, the heat equation is solved using the backward Euler method for three scenarios including a test case. The solution of the known test case is then compared against its analytical solution.

## I. INTRODUCTION

In mathematics, finite-difference methods (FDM) provides series of recurrence relations for the derivatives of a partial differential equation (PDE) by discretising them into difference equations, essentially allows for the approximation of the solutions and hence solve it by linear algebra techniques. As a result, the ability to recast the recurrence relations into algebraic equation makes it suitable for the PDE to be solved on a modern computer, and hence FDM(s) remain the dominating approach to numerically solving PDE(s).

## II. SOLVING LAPLACE'S EQUATION

Consider a physics experiment where

The task is to solve the Laplace's equation by writing an iterative algorithm using the finite difference representation which comes from its two-dimensional Taylor expansion. And then the discretised differences can be iterated by either the Jacobi or Gauss-Seidel method. It is required that we first solve it for a simple known case, which was chosen to be a wire in a box since it has a closed-form solution expressed in terms of a Fourier series which can be found in common literature. Since the true solution is technically the sum of infinite terms of the Fourier series solution, by choosing a huge number of terms in the sum we can ensure that the error analysis can be done relative to an extremely good approximation of the true solution.

### A. KNOWN CASE: LINE CHARGE IN A GROUNDED BOX

In this case the wire in the box represents a line charge, for which its ceiling is kept at a constant potential of 1000V, with its both edges and bottom grounded. These are the corresponding boundary conditions for this scenario. Since the grid of the simulation was initiated as a matrix containing elements of zero anyway, there was no need to explicitly code in the grounded boundary condition, which leaves the only boundary condition with fixing the line at a constant potential.

It is clearly shown in FIG.1 that the electric field lines are diverging out in a non-uniform manner, which is expected since all the edges of the box are grounded. As a consequence the equipotential lines are also reflected correctly, radiating out non-uniformly and curves the further it travel. By solving

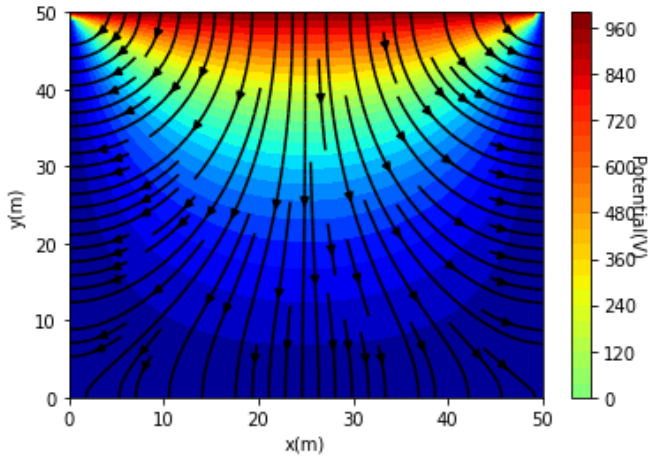


FIG. 1. A heatmap of a line charge with constant potential of 1000V. The descent of colour gradient represents the equipotential lines, with its magnitude shown on the colourmap. The streamline plot indicates the corresponding electric field and its direction.

Laplace's equation by means of separation of variables, it can be shown that the most general form of solution is a linear superposition of all of its solution, given by

$$\phi(x,y) = \sum_{n=1}^{\infty} \phi_n \sin\left(\frac{n\pi}{L}x\right) \sinh\left(\frac{n\pi}{L}y\right). \tag{1}$$

The constant $\phi_n$ can then be calculated by using the "Fourier trick"[1] whilst satisfying the boundary condition of $\phi(x, y = L) = 1000$V, giving

$$\phi(x,y) = \sum_{n=1}^{\infty} \frac{4 * 1000}{n\pi} \sin\left(\frac{n\pi}{L}x\right) \frac{\sinh(n\pi y/L)}{\sinh(n\pi)}. \tag{2}$$

as the final solution[2]. Since Eq.(2) is an infinite sum, this means that the summation will have to be terminated when implemented as an algorithm. To justify the use of Fourier series solution as "accurate" answer, its shortcomings must first be discussed. At first it may seem like to get an accurate final answer, one will just have to take as many terms of the sum as possible. However, in practice the convergence of the sum could be computationally slow for a desirable accuracy, which could then introduce round-off error. Moreover, in the limit of

large $n$ python does not deal with the sinh functions of Eq.(2) very well, and will just end up returning NaN as an overflow error for a tested value of n bigger than 114.

If the convergence of the sinh functions in Eq.(2) can be known, then the computational overflow error can then be overcome. It is natural then to take the limit of the division of the two sinh function by first expressing them in terms of exponential, as n tends towards infinity:

$$\lim_{n\to\infty} \frac{\sinh(n\pi y/L)}{\sinh(n\pi)} = \lim_{n\to\infty} \frac{e^{n\pi(y/L-1)} - e^{-n\pi(y/L+1)}}{1 - e^{-2n\pi}} = e^{n\pi(y/L-1)} \tag{3}$$

Hence for $n > 114$, the overflow error has been taken into consideration in the code by replacing the division of sinh in Eq.(3) by its exponential limit. The final problem with using Fourier series solution as the relative measure to our relaxed algorithmic solution is that a Fourier series only converges towards the average of the left and right for which the solution is discontinuous such as the edges of the box where the boundary conditions apply. This leads to what is called the Gibbs phenomenon which occurs when a piece-wise continuous function is being represented by a Fourier series of finite terms. At the boundary, rather than diminishing to zero the series instead starts to have oscillatory behaviour and tends to overshoot at the corner where the discontinuity happens. The overshoot does not go away for large $n$, but can be reduced however to a finite limit. Finally, the use of Fourier series solution as our "true solution" can then be justified if decisions are made to avoid these aforementioned shortcomings. Therefore to avoid the oscillating values by the effects of Gibbs phenomenon, we avoid comparing values between 2 solutions at the boundary of the solution where the effects tend to overshoot. Next, pick a total number of term for which the solution is smooth.

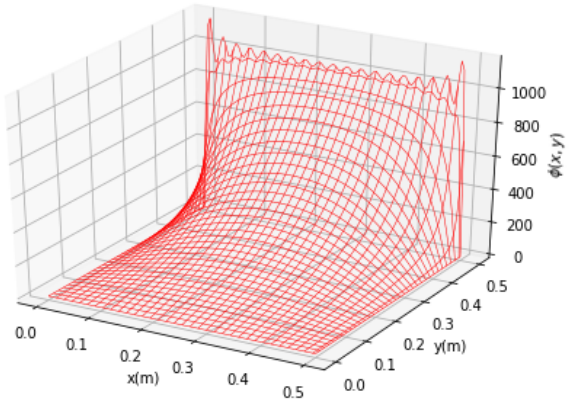


FIG. 2. The Fourier series solution of the Laplace equation for a line charge inside a grounded box, as given by Eq.(2), plotted across the x-y which spans the box for n = 20. Here the z-dimension demonstrates the oscillatory motion at the edges, thereby demonstrating the Gibbs phenomenon. Larger oscillations can be seen happening at the corner.

The amount of terms to be included in the summation was chosen to be 40000 such that the whole function is sufficiently smooth. On top of that the slice of investigation was chosen to be $y = 0.25$ such that it is away from the edges as much as possible. It can be seen from FIG.3 that for this particular slice the potential, $\phi(x, y = 0.25)$, from both the analytical and Gauss-Seidel relaxation solution actually lie very closely to each other, with the analytical solution just slightly overshooting the other. This could be due to rounding errors in the analytical solution or that somehow the GS solution did not manage to relaxed to its final solution.

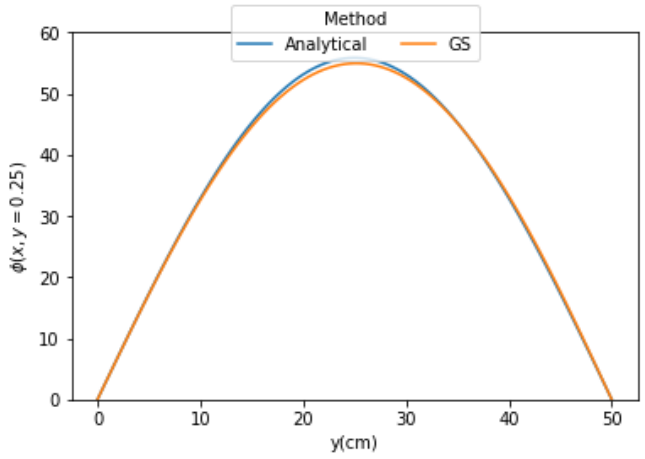


FIG. 3. The Fourier series solution of the Laplace equation for a line charge inside a grounded box alongside the final relaxed solution by the Gauss-Seidel method plotted across the x-axis of the box for y = 0.25m.

### B. PARALLEL PLATE CAPACITOR

For the second task the potential and electric field of a parallel charge capacitor is calculated and plotted using both the Gauss-Seidel and Jacobi method. Both methods are very similar so it was expected that they should both relax to the same final solution, with a variation in amount of iteration that is needed for convergence. A convergence condition is set up to stop the iterations of both method as soon as reach a certain tolerance level, which is set for 0.00001% for both so that their convergence iteration can be compared. The potential and electric field plotted using both Gauss-Seidel and Jacobi methods for a parallel plate capacitor of length 20cm and a plate separation of 9cm are shown in FIG.4 and FIG.5 correspondingly. Since they both converge to an identical solution, their plots look the same. As expected the horizontal slice of potential between both plates of opposite potential, 1000V and -1000V, should be 0. The quiver plot also demonstrated correctly that the field lines are flowing from the potential with positive to the negative plate. From FIG.5, it can be seen that that electric field lines are constant closer to the centre between two plates, and it starts to curve towards the end of the plates.

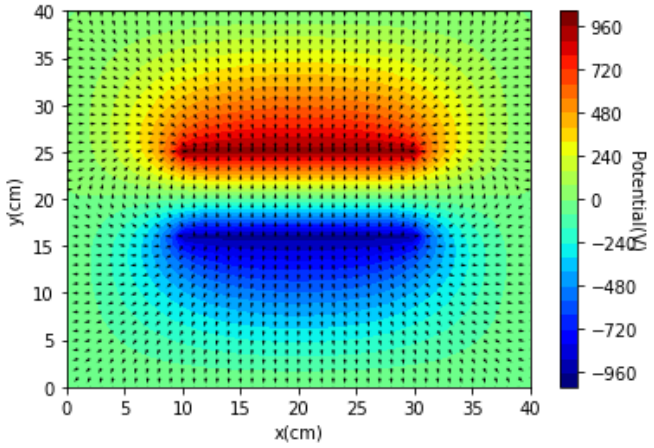


FIG. 4. The potential of a parallel plate capacitor with length 20cm and plate separation of 9cm. A quiver plot is overlayed on top of it to show the grid density and the direction of electric field at each point.

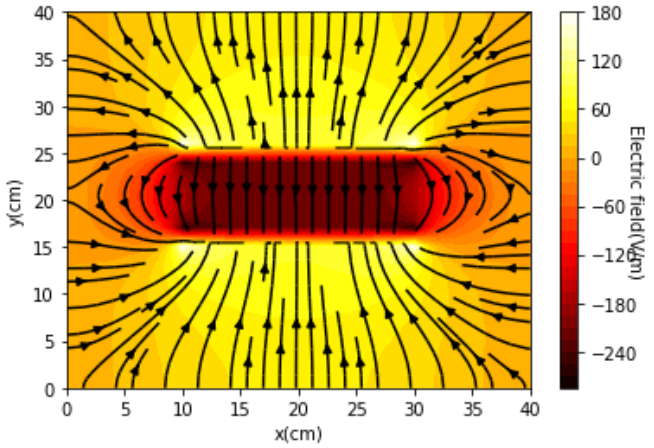


FIG. 5. Similar plot as FIG.4 except the electric field is plotted instead. A streamline plot is overlayed on top of it to show the direction of bulk field lines and the colour gradient indicates the magnitude of the E-field.

## III. SOLVING THE HEAT DIFFUSION EQUATION

For this task the technique of backward-Euler propagation is used to solve the diffusion of equation,

$$\frac{\partial \phi}{\partial t} = \alpha \nabla^2 \phi = \frac{k}{\rho c_p} \nabla^2 \phi \tag{4}$$

for heat on a rod, where $\alpha$ is the thermal diffusivity, which is equal to the thermal conductivity, $k$, divided by density and specific heat capacity at constant pressure. The diffusion can once again be recast in to finite difference form, which can be expressed as a system of linear equation in matrix form:

$$\mathbf{A} \cdot \begin{pmatrix} \vdots \\ \phi'(x_{i-1}) \\ \phi'(x_i) \\ \phi'(x_{i+1}) \\ \vdots \end{pmatrix} = \begin{pmatrix} \vdots \\ \\ \phi(x_i) \\ \\ \vdots \end{pmatrix} \tag{5}$$

where **A** a tridiagonal and conventionally Toeplitz matrix with main diagonal having $N$ elements of $(1 + 2\kappa, ..., 1 + 2\kappa)$ and the lower and upper diagonal elements having $(N - 1)$ elements of $(-\kappa, ..., -\kappa)$. Here $\kappa = \alpha dt/dx^2$ where $dt$ and $dx$ are the time and spatial steps for the finite differences respectively. These are the main constants which propagates the solution for each iteration. Since for this question the starting temperatures of the start and the end of the rod are known, depending on what these the boundary conditions are, the first or last of the elements of the upper, lower and main diagonal matrix would be changed. For example, it is obvious that the first element of the main diagonal matrix should be 1 if the temperature of the head of the head is a known constant. A quick way to compute the Toeplitz matrix would be to avoid storing the already know elements of zeros anywhere outside of the main three diagonal matrices. By initiating the main 3 diagonal elements manually and create a tridiagonal out of it using the linalg library and fill every other element with zero, with (N+1) unknown we will only require a storage requirements of $(N+1)^2$

The algorithm is first implemented on a known test case with both ends of the rod submerged into an ice bath, with the body of the rod initially starting at 20°C. The plot is shown in FIG.6. It can be seen from the plotting the first iteration

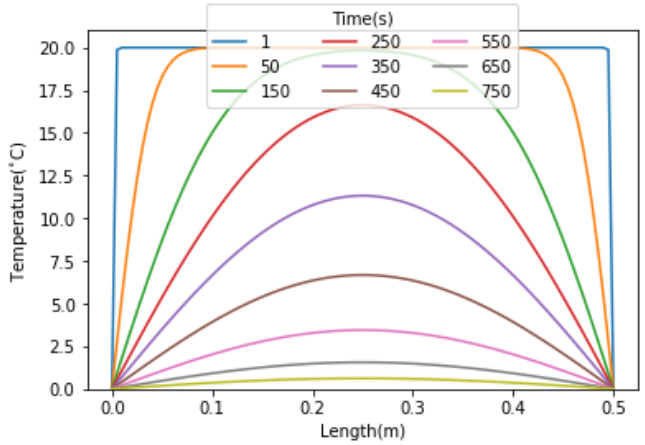


FIG. 6. The heat diffusion of a rod with both end submerged in an ice bath at time T = 0.

at $T$=1s that the algorithm does indeed work. Since at $T$=1s strictly only the second element along the temperature matrix would have had iterated, therefore the whole temperature distribution is strictly a square wave function. For this specific case, there exists an analytical that the numerical solution can be compared to. The Fourier series solution of this scenario is

given by:

$$T(x,t) = \sum_{n=1}^{\infty} \frac{4T_0}{(2n-1)\pi} \sin\left(\frac{(2n-1)\pi x}{L}\right) e^{-(\sqrt{\alpha}(2n-1)\pi/L)^2 t} \tag{6}$$

where $T_0$ is the initial temperature of the rod which is 20° in this case. With an analytical solution the same analysis as FIG.3 can be done. With the analytical solution taken up to a sum of 1000 terms, it could reasonably approximate the "true solution". The error analysis is done by summing up all the absolute differences between all the elements of the FD and analytical solution, and then a mean error value is taken out of all the error values. The result is plotted for several different final time and is shown in FIG.7. Parts of FIG.7 corresponds to the time in FIG.6 for the selection of times between which the rod is completely cooled to zero.

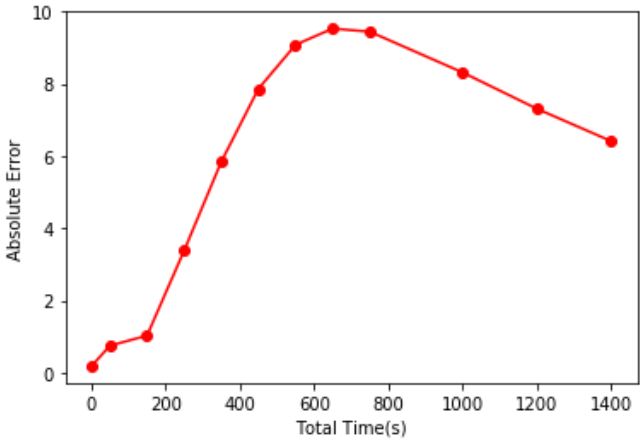


FIG. 7. The absolute erorr plotted for a total time T of 1, 50, 150, 250, 350, 450, 550, 650, 750, 1000, 1200, 1400 seconds respectively.

As expected, the absolute error would start decreasing approximately after 750s which is when whole temperature of the bar reaching zero. Since both solutions approaches zero everywhere on the bar, it makes sense that their element differences will also be very small, thereby tending the error to zero.

The same algorithm is repeated for the calculation of two different scenarios one with an insulated rod with the head of rod in furnace and the other with one end submerging in an ice bath and the other in a furnace. The results are shown in Comparing FIG.7 to FIG. 8, the time for which

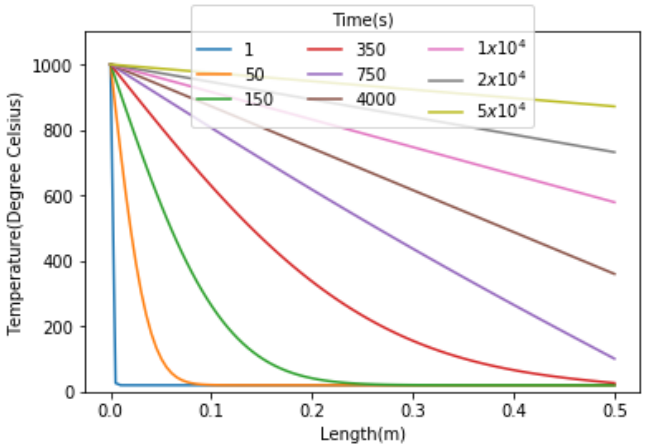


FIG. 8. The heat distribution along an adiabatic rod with its head in a furnace at a different final time T.

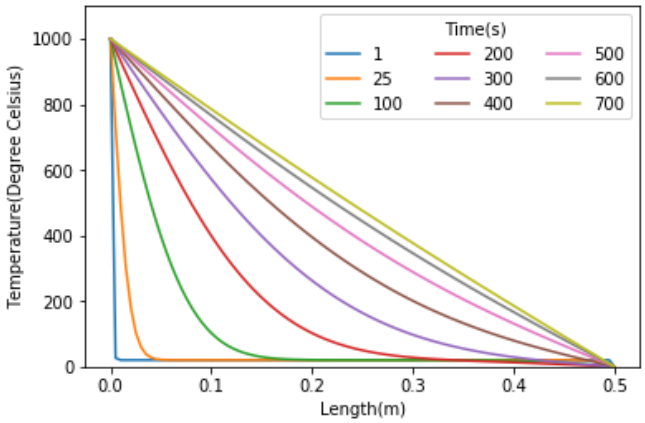


FIG. 9. The heat distribution along a rod with its head in a furnace and its tail in an ice bath at 0°C for a different final time T.

## IV. REFERENCES

[1] Griffiths. D. J (1999) *Introduction to Electrodynamics* Upper Saddle River, N.J.: Prentice Hall.

[2] Landau. H. R, Paez. J. M and Bordeianu. C. C (2015) *Computational Physics: Problem solving with Python* Wiley-VCH.